



CHORUS

This is the accepted manuscript made available via CHORUS. The article has been published as:

Pattern Formation with Trapped Ions

Tony E. Lee and M. C. Cross

Phys. Rev. Lett. **106**, 143001 — Published 5 April 2011

DOI: [10.1103/PhysRevLett.106.143001](https://doi.org/10.1103/PhysRevLett.106.143001)

Pattern formation with trapped ions

Tony E. Lee and M. C. Cross

Department of Physics, California Institute of Technology, Pasadena, California 91125, USA

Ion traps are a versatile tool to study nonequilibrium statistical physics, due to the tunability of dissipation and nonlinearity. We propose an experiment with a chain of ions, where dissipation is provided by laser heating and cooling, while nonlinearity is provided by trap anharmonicity and beam shaping. The dynamics are governed by an equation similar to the complex Ginzburg-Landau equation, except that the reactive nature of the coupling leads to qualitatively different behavior. The system has the unusual feature of being both oscillatory and excitable at the same time. The patterns are observable for realistic experimental parameters despite noise from spontaneous emission. Our scheme also allows controllable experiments with noise and quenched disorder.

PACS numbers:

Pattern formation is the emergence of structure in a nonlinear medium far from equilibrium [1, 2]. This phenomenon occurs in many settings, including fluids, chemical reactions, plasmas, and biological tissues. In traditional pattern-forming systems, the collective behavior is set by the material properties, and theoretical descriptions are often phenomenological. For example, in the Belousov-Zhabotinsky reaction, the concentrations of chemical reagents oscillate in time and produce traveling waves. It is a complicated reaction involving many intermediate states and rate constants. Hence, it is difficult to experimentally control the behavior of the system.

On the other hand, ion traps allow an unprecedented level of control using optical and electrostatic forces and have led to impressive experiments in quantum computing [3, 4] and quantum simulation [5, 6]. In this paper, we show how ions are also useful for studying pattern formation. The advantage of using ions here is the ability to tune dissipation and nonlinearity *in situ*, thereby having more experimental control and being able to see different effects within the same system.

We show how patterns arise in a chain of ions driven far from equilibrium. The collective dynamics are governed by an equation similar to the complex Ginzburg-Landau equation, which is one of the most studied equations in physics. However, the presence of only reactive coupling in the ion chain leads to novel behavior: while other systems are either oscillatory or excitable, the ion chain can be both at the same time. Our scheme is also useful for studying synchronization and Anderson localization. Our work is motivated by recent experiments on the nonlinear dynamics of single ions: a phonon laser [7, 8] and a Duffing oscillator [9]. The model studied here can also describe an array of nanomechanical resonators [10, 11].

First we describe the proposed experimental setup. A linear Paul trap uses an RF electric field for radial confinement and a DC field for axial confinement [3]. We use a segmented trap, which has many DC electrodes in order to create many trapping regions [12], and thereby make a chain of ions, each in its own potential well. By changing the DC voltages, one can tune the shape of the

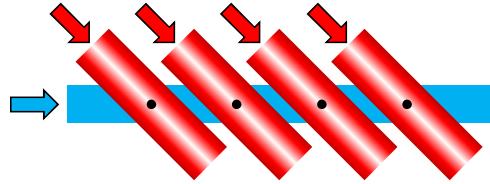


FIG. 1: Chain of ions, each damped by a red-detuned beam and excited by a blue-detuned beam. The blue beam is along the ion chain, while the red beams are at an angle. The intensity of the red beams is lowest at the trap center. Each ion is in its own anharmonic DC potential well (not shown).

potential for each ion and thus control the nonlinearity [13, 14]. Let x be the axial displacement of an ion from its trap center, d the distance between trap centers, ω_o the harmonic trap frequency, and α_o the coefficient of the anharmonic quartic term in the trap potential.

We apply near-resonant laser beams to heat and cool each ion (Fig. 1). When the laser frequency is above resonance (blue-detuned), the ion feels an anti-damping force due to the Doppler effect. When the laser frequency is below resonance (red-detuned), the ion feels a damping force [15]. We apply a blue-detuned beam in the axial direction along the ion chain. For each ion, we also apply a red-detuned beam at an angle ϕ with respect to the trap axis. The red beam is shaped so that the intensity is lowest at the trap center. The ion is then heated near the center and increasingly cooled away from the center, so the ion oscillates with a large amplitude, determined by the balance of heating and cooling. The dissipation is easily tuned by changing the beam intensity.

We use a singly-ionized, two-level atom of mass m with a dipole transition of wavelength $\lambda = 2\pi/k$ and linewidth γ . Each red and blue beam has detuning $-\Delta\omega$ and $+\Delta\omega$ and intensity I_R and I_B , respectively. Let I_s be the saturation intensity. All beams have the same polarization.

We use low laser intensities so that the ion is unsaturated. We assume the radial motion is cooled near the Doppler limit (due to the projection of the red beams),

so that the Doppler shift is due mainly to the axial motion. For mathematical convenience, we use counter-propagating beams (but in practice one would use single beams). The total optical force on an ion is [7],

$$\frac{8\hbar k^2 \gamma^3 \Delta\omega}{(\gamma^2 + 4\Delta\omega^2)^2} \left(-\frac{I_R}{I_s} \cos^2 \phi + \frac{I_B}{I_s} \right) \dot{x}, \quad (1)$$

under the additional assumptions $k|\ddot{x}| \ll \gamma^2/4$ and $k|\dot{x}| \ll \Delta\omega$. To get position-dependent damping, we choose to vary I_R quadratically along the trap axis,

$$I_R(x) = \left(\frac{x}{\ell \cos \phi} \right)^2 I_B, \quad (2)$$

where ℓ is the characteristic length of the intensity gradient. The intensity profile does not need to take this form or even be symmetric. In fact, a different profile may lead to interesting higher-order terms in Eq. (5) [16].

The ions are coupled through Coulomb repulsion. If the displacements are small relative to the inter-ion distance ($\ell \ll d$), the interaction is linear, and the free-space coupling decreases with the cube of the distance. Numerically, we find that interactions farther than the nearest neighbor do not affect the overall dynamics much, so we assume only nearest-neighbor interactions. The equations of motion are,

$$0 = \frac{d^2}{dt^2} x_n + \omega_o^2 x_n + \alpha_o x_n^3 - \mu \left[1 - \left(\frac{x_n}{\ell} \right)^2 \right] \frac{d}{dt} x_n + \frac{2k_e e^2}{md^3} [(x_n - x_{n-1}) + (x_n - x_{n+1})] + \chi_n(t), \quad (3)$$

$n = 1, \dots, N$, where k_e is the Coulomb constant, e is the proton charge, μ is the damping coefficient,

$$\mu = \frac{8\hbar k^2 \gamma^3 \Delta\omega I_B / I_s}{m(\gamma^2 + 4\Delta\omega^2)^2}, \quad (4)$$

and $\chi_n(t)$ is the noise. In this scheme, the inherent source of noise is spontaneous emission, since each emission causes a momentum kick $\hbar k$ in a random direction.

We work in the regime where the nonlinearities and interactions are small perturbations to the harmonic motion. We write $x_n(t) = 2\ell \text{Re}[A_n(t)e^{-i\omega t}]$, so that the complex amplitude A_n encodes the slowly varying amplitude and phase of the underlying harmonic oscillations. In the Supplemental Material, we find the amplitude equation,

$$\frac{dA_n}{dt} = ib(-2A_n + A_{n-1} + A_{n+1}) - (1 + ic)|A_n|^2 A_n + A_n + [\eta_n^R(\bar{t}) + i\sigma_n^R(\bar{t})]A_n + [\eta_n^B(\bar{t}) + i\sigma_n^B(\bar{t})], \quad (5)$$

$$b = \frac{2k_e e^2}{\nu md^3 \omega_o^2}, \quad c = \frac{3\alpha_o \ell^2}{\nu \omega_o^2}, \quad \nu = \frac{8\hbar k^2 \gamma^3 \Delta\omega I_B / I_s}{m\omega_o(\gamma^2 + 4\Delta\omega^2)^2}, \quad (6)$$

where $\bar{t} = \mu t/2$ is rescaled time, b is the coupling, and c relates how an ion's amplitude affects its frequency. We stress that b and c are directly related to experimental settings. In the absence of coupling, each ion oscillates with amplitude $|A| = 1$, which corresponds to an amplitude of 2ℓ in x . The noise functions are due to spontaneous emission and represent scattering by the red beams (η^R, σ^R) and blue beams (η^B, σ^B),

$$\langle \eta_m^R(\bar{t}) \eta_n^R(\bar{t}') \rangle = \frac{1}{3} \langle \sigma_m^R(\bar{t}) \sigma_n^R(\bar{t}') \rangle = \frac{H \delta(\bar{t} - \bar{t}') \delta_{mn}}{\cos^2 \phi} \quad (7)$$

$$\langle \eta_m^B(\bar{t}) \eta_n^B(\bar{t}') \rangle = \langle \sigma_m^B(\bar{t}) \sigma_n^B(\bar{t}') \rangle = H \delta(\bar{t} - \bar{t}') \delta_{mn} \quad (8)$$

$$H = \frac{\hbar(\gamma^2 + 4\Delta\omega^2)}{96m\omega_o^2 \ell^2 \Delta\omega}, \quad (9)$$

where H is a dimensionless measure of the noise.

We now examine the spatiotemporal properties of Eq. (5), ignoring the effect of noise for now. The equation is symmetric under the transformation $b, c, A_n \rightarrow -b, -c, A_n^*$. In the continuum limit, let $A_n \rightarrow A(X)$:

$$\frac{dA}{dt} = A + ib \frac{d^2 A}{dX^2} - (1 + ic)|A|^2 A. \quad (10)$$

This is similar to the complex Ginzburg-Landau equation (CGLE) [17], except that the coefficient of $d^2 A/dX^2$ is purely imaginary. This is because the Coulomb force is reactive, while the CGLE includes both reactive and dissipative interactions. This greatly modifies the behavior.

According to Eq. (10), a plane wave solution $A(X, \bar{t}) = F e^{i(QX - \omega \bar{t})}$ satisfies $F = 1$ and $\omega = bQ^2 + c$. By linearizing around this solution [2], we find that the condition for stability is $bc \geq 0$, and as long as this is fulfilled, there is no restriction on the wave number Q . Since Eq. (10) is in the continuum limit, we expect long wavelength waves (wavelength at least several ions) when $bc \geq 0$.

When $bc \leq 0$, it turns out that Eq. (5) allows short wavelength waves that are not captured in the continuum limit. Define $\hat{A}_n = -A_n^*$ for even n and $\hat{A}_n = A_n^*$ for odd n and consider the continuum limit of the transformed system. A plane wave $\hat{A}(X) = \hat{F} e^{i(\hat{Q}X - \hat{\omega} \bar{t})}$ satisfies $\hat{F} = 1$ and $\hat{\omega} = b(\hat{Q}^2 - 4) - c$, and the stability condition for long-wavelength waves is $bc \leq 0$. A long wavelength wave in \hat{A} corresponds to a very short wavelength wave in A .

Therefore, Eq. (5) has stable plane waves for all values of b and c : long wavelength for $bc \geq 0$ and short wavelength for $bc \leq 0$. This behavior is different from the CGLE, which has stable plane waves for $bc > -1$ and is otherwise chaotic [17]. Another difference is that in the CGLE, only a band of Q is stable.

However, boundary conditions affect the selection of plane waves. With periodic boundary conditions, the wave number (Q or \hat{Q}) is a multiple of $2\pi/N$. Open boundary conditions are simpler to implement and are equivalent to setting $\frac{dA}{dX} = 0$ at the boundaries. Thus when $bc > 0$, the only allowed plane wave is the $Q = 0$ wave, in which the ions are uniformly in-phase (Fig. 2a).

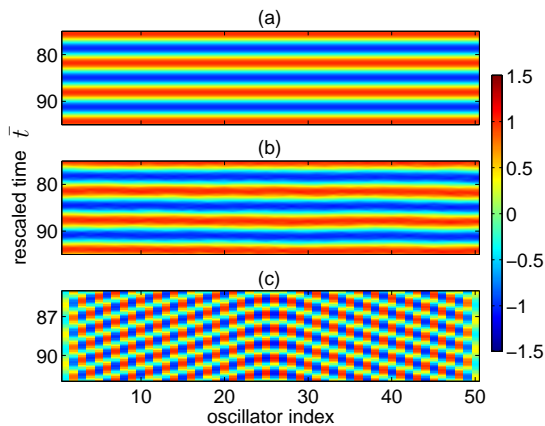


FIG. 2: Spacetime plot of chain of 50 ions with nearest neighbor interactions and open boundaries. $\text{Re } A$ is plotted using the color scale in the side bar. A is the complex amplitude of the underlying harmonic oscillations. (a) $b = 1$ and $c = 1$ showing uniform phase synchrony. (b) Same, but with the expected noise from spontaneous emission. (c) $b = 1$ and $c = -1$ showing anti-phase structure.

(This also occurs in the Belousov-Zhabotinsky reaction in the absence of spatial inhomogeneities [2]). One can induce $Q \neq 0$ waves by, for example, changing the trap frequency ω_o of one ion. The $bc < 0$ case is different, because open boundary conditions mean setting $\tilde{A} = 0$ at the boundaries. The final state is not a pure plane wave but a more complicated structure, in which the ions are almost uniformly anti-phase (Fig. 2c).

We now examine the dynamics of two coupled ions, expanding on previous work [18, 19]. First write Eq. (5) in terms of the real amplitudes r_1, r_2 and phase difference $\Delta\theta = \theta_2 - \theta_1$, where $A_n = r_n e^{-i\theta_n}$,

$$\frac{d\Delta\theta}{d\tilde{t}} = (r_2^2 - r_1^2) \left(c + \frac{b}{r_1 r_2} \cos \Delta\theta \right) \quad (11)$$

$$\frac{dr_1}{d\tilde{t}} = (1 - r_1^2)r_1 + br_2 \sin \Delta\theta \quad (12)$$

$$\frac{dr_2}{d\tilde{t}} = (1 - r_2^2)r_2 - br_1 \sin \Delta\theta. \quad (13)$$

This system is symmetric under the transformations $\{r_1, r_2, \Delta\theta \rightarrow r_2, r_1, -\Delta\theta\}$, $\{c, \Delta\theta \rightarrow -c, \pi - \Delta\theta\}$, and $\{b, \Delta\theta \rightarrow -b, \pi + \Delta\theta\}$. There are fixed points at $(\Delta\theta, r_1, r_2) = (0, 1, 1)$ and $(\pi, 1, 1)$, corresponding to in-phase and anti-phase motion. Another set of fixed points corresponds to roots of a quartic polynomial of r_1^2 ,

$$0 = (c^2 - 1)^2 r_1^8 - (c^2 - 1)(c^2 - 3)r_1^6 - (c^2 - 3)r_1^4 - (b^2 + 1)(c^2 + 1)r_1^2 + b^2(b^2 + 1), \quad (14)$$

which may be solved numerically. The bifurcation diagram is quite rich: as b and c change, saddle-node, pitchfork, and Hopf bifurcations appear, disappear, and change critically. An example is shown in Fig. 3a. For

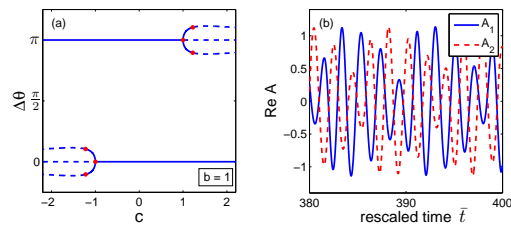


FIG. 3: System of two oscillators with $b = 1$. (a) Bifurcation diagram as c varies. There are supercritical pitchfork bifurcations at $(c, \Delta\theta) = (-1, 0)$ and $(1, \pi)$. There are supercritical Hopf bifurcations at $(1.22, 2.82)$, $(1.22, 3.47)$, $(-1.22, -0.32)$, and $(-1.22, 0.32)$, which give rise to stable limit cycles (not shown). Solid and dashed lines denote stable and unstable fixed points, respectively. (b) A limit cycle at $c = 1.4$.

some values of b and c , there are supercritical Hopf bifurcations to stable limit cycles, in which the amplitudes and relative phase oscillate (Fig. 3b). The system is at least bistable for $|c| < |b|$, but certain values of b and c have four stable fixed points.

As N increases, there are still in-phase ($\Delta\theta = 0$) and anti-phase ($\Delta\theta \approx \pi$) fixed points, although the region of multistability in bc space shrinks. For $|c| \lesssim |b|$, there are also multiple stable limit cycles, in which the entire chain has the same average frequency or the chain is divided into regions of different frequencies.

A large ion chain is excitable in a novel way. An excitable medium has the property that the uniform state is stable to weak perturbations, but a perturbation that exceeds a threshold grows rapidly and then decays. For example, when a small voltage is applied to a neuron's membrane, the neuron remains in the resting state. But if the applied voltage is large enough, it triggers a pulse of high voltage (an action potential), which travels along the length of the cell. Usually, a medium is either oscillatory or excitable [2]. For example, a neuron is excitable but not oscillatory, since the membrane voltage does not oscillate in the absence of an action potential. On the other hand, the CGLE describes only oscillatory media because there is no threshold. However, the ion chain is both oscillatory and excitable *at the same time*. Suppose that $bc > 0$ and the chain is in the $Q = 0$ state (in-phase), with N large. We perturb the first ion A_1 by δA . The $Q = 0$ state is linearly stable so a small perturbation decays away. But if δA is greater than a threshold, it generates a localized pulse of anti-phase oscillations (Fig. 4). The pulse travels across the system, bouncing off the boundaries until it decays.

It is surprising that the ion chain is excitable, since excitable media are usually reaction-diffusion systems. Here, the pulse is made of an alternating phase structure instead of an increased chemical concentration. The excitability can be intuitively understood from the fact that when $bc > 0$ and $|c| \lesssim |b|$, both in-phase and anti-

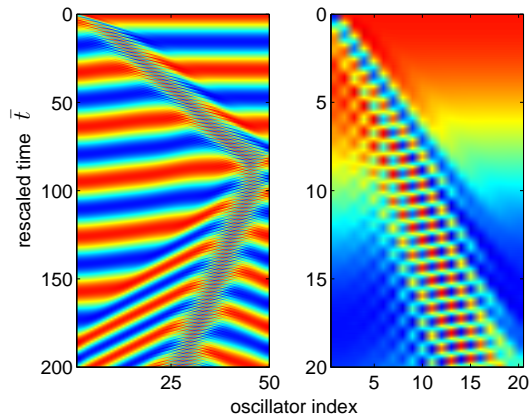


FIG. 4: Spacetime plot of $\text{Re } A$ for chain of 50 ions showing an excitation pulse for $b = 1$ and $c = 0.2$. Perturbing the first oscillator beyond a threshold generates a pulse of anti-phase oscillation. The initial conditions were $A_1 = -1$ and $A_n = 1$ for the rest. The right panel is a zoomed-in view. Color scale is the same as in Fig. 2.

phase oscillations may be stable for small chains, while only in-phase oscillation is stable for large chains. Thus, a local region within a large chain may be anti-phase for a short amount of time. We attribute the excitability to the reactive nature of the coupling, since the CGLE is not excitable. A mathematical description of this phenomenon is left open for future work: it would be interesting to calculate the threshold and pulse shape as a function of b and c .

The patterns described above would be observable above the noise from spontaneous emission for realistic experimental settings that satisfy all the theoretical assumptions. For example, the ion $^{24}\text{Mg}^+$ has an $S_{1/2} - P_{3/2}$ dipole transition of wavelength $\lambda = 279.6$ nm and linewidth $\gamma/2\pi = 42$ MHz. Letting $\omega_o/2\pi = 100$ kHz, $I_B/I_s = 0.05$, $\Delta\omega = 6\gamma$, $\phi = \pi/4$, $\ell = 30$ μm , $\alpha_o/4\pi^2 = 10^{15}$ Hz^2/m^2 , and $d = 500$ μm , one finds $b = 1.0$, $c = 1.1$, and $H = 5 \times 10^{-4}$. Figure 2b shows that the $Q = 0$ state is clearly visible above the noise. Also, since many experiments are already using large-scale traps for quantum information [12], it should be straightforward to implement our scheme with many ions.

In the experiment, one can measure the amplitude and phase of A_n by recording when and where the ions scatter photons [8, 9]. Changes in A_n occur on a time scale $t \sim 1/\mu$, which is much slower than that of the harmonic oscillation ($\sim 1/\omega_o$). Thus, one can observe dynamical effects, such as limit cycles and excitation pulses. The entire bc space can be explored by, for example, tuning the parameters I_B and α_o .

It would be interesting to turn up the noise to see what happens. It is known that adding noise to a spatially extended system may have nontrivial effects [20]. However, it is usually experimentally difficult to make the noise

fluctuate not only in time but in space as well. In our scheme, the noise for each ion is independent and may be easily tuned by changing the detuning $\Delta\omega$ in Eq. (9). One could observe, for example, noise-induced transitions between stable fixed points in a small chain.

Another interesting use of the tunability is to study the effect of quenched disorder. A previous work studied the mean-field version of Eq. (5) with random harmonic frequencies ω_o and found that as b and c change, the system undergoes continuous and discontinuous phase transitions between the unsynchronized and synchronized states [10, 11]. It would be interesting to study the lower-dimensional versions. We note that synchronization of disparate oscillators is an important topic throughout science [21, 22]. Furthermore, when the variance of ω_o is small, Eq. (5) may be mapped via the Cole-Hopf transformation to the Schrödinger equation for a particle in a random potential [23, 24]. The resulting pattern formation reflects the phenomenon of Anderson localization.

We thank H. Häffner for helpful comments. This work was supported by Boeing and NSF grant DMR-1003337.

-
- [1] M. C. Cross and P. C. Hohenberg, *Rev. Mod. Phys.* **65**, 851 (1993).
 - [2] M. C. Cross and H. Greenside, *Pattern Formation and Dynamics in Nonequilibrium Systems* (Cambridge University Press, Cambridge, 2009).
 - [3] D. Leibfried et al., *Rev. Mod. Phys.* **75**, 281 (2003).
 - [4] H. Häffner et al., *Physics Reports* **469**, 155 (2008).
 - [5] K. Kim et al., *Nature* **465**, 590 (2010).
 - [6] A. Friedenauer et al., *Nature Physics* **4**, 757 (2008).
 - [7] K. Vahala et al., *Nature Physics* **5**, 682 (2009).
 - [8] S. Knünz et al., *Phys. Rev. Lett.* **105**, 013004 (2010).
 - [9] N. Akerman et al., *Phys. Rev. A* **82**, 061402(R) (2010).
 - [10] M. C. Cross et al., *Phys. Rev. Lett.* **93**, 224101 (2004).
 - [11] M. C. Cross et al., *Phys. Rev. E* **73**, 036205 (2006).
 - [12] D. Kielpinski et al., *Nature* **417**, 709 (2002).
 - [13] W. K. Hensinger et al., *Appl. Phys. Lett.* **88**, 034101 (2006).
 - [14] G.-D. Lin et al., *Europhys. Lett.* **86**, 60004 (2009).
 - [15] H. J. Metcalf and P. van der Straten, *Laser Cooling and Trapping* (Springer, New York, 1999).
 - [16] W. van Saarloos and P. C. Hohenberg, *Physica D* **56**, 303 (1992).
 - [17] I. S. Aranson and L. Kramer, *Rev. Mod. Phys.* **74**, 99 (2002).
 - [18] A. Kuznetsov et al., *Physica D* **238**, 1203 (2009).
 - [19] M. Grau, Senior thesis, California Institute of Technology (2009).
 - [20] F. Sagués et al., *Rev. Mod. Phys.* **79**, 829 (2007).
 - [21] A. S. Pikovsky, M. Rosenblum, and J. Kurths, *Synchronization: A Universal Concept in Nonlinear Science* (Cambridge University Press, New York, 2001).
 - [22] J. A. Acebrón et al., *Rev. Mod. Phys.* **77**, 137 (2005).
 - [23] H. Sakaguchi et al., *Prog. Theor. Phys.* **79**, 1069 (1988).
 - [24] B. Blasius and R. Tönjes, *Phys. Rev. Lett.* **95**, 084101 (2005).